ACS APPLIED MATERIALS & INTERFACES

Letter

www.acsami.org

Electrodeposited MnO_x/PEDOT Composite Thin Films for the Oxygen Reduction Reaction

Julian A. Vigil, Timothy N. Lambert,* and Kaitlyn Eldred

Department of Materials, Devices & Energy Technologies, Sandia National Laboratories, Albuquerque, New Mexico 87185, United States

Supporting Information

ABSTRACT: Manganese oxide (MnO_x) was anodically coelectrodeposited with poly(3,4-ethylenedioxythiophene) (PEDOT) from an aqueous solution of $Mn(OAc)_2$, 3,4-ethylenedioxythiophene, $LiClO_4$ and sodium dodecyl sulfate to yield a MnO_x/PEDOT composite thin film. The MnO_x/PEDOT film showed significant improvement over the MnO_x only and PEDOT only films for the oxygen reduction reaction, with a >0.2 V decrease in onset and half-wave overpotential and >1.5 times increase in current density. Furthermore, the MnO_x/PEDOT films were competitive with commercial benchmark 20% Pt/C, outperforming it in the half-wave ORR region and exhibiting better electrocatalytic selectivity for the oxygen reduction reaction upon methanol exposure. The high activity of the MnO_x/PEDOT composite is attributed to synergistic charge transfer capabilities, attained by coelectrodepositing MnO_x with a conductive polymer while simultaneously achieving intimate substrate contact.

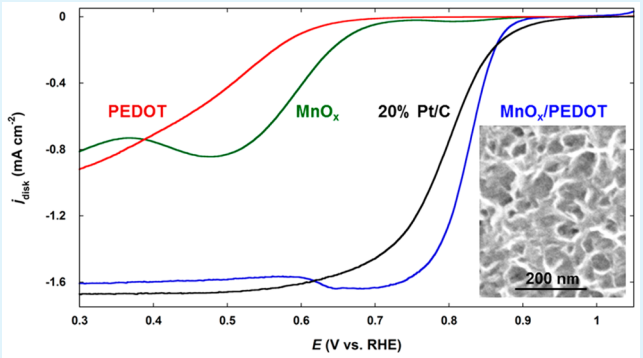

KEYWORDS: *catalysis, oxygen reduction reaction, manganese oxide, PEDOT, electrodeposition*

As one of the key electrochemical reactions in energy storage and conversion applications, the efficiency of the oxygen reduction reaction (ORR) is crucial to next-generation devices. High overpotentials are associated with the complex, four-electron transfer of the ORR, increasing operating potentials for devices like fuel cells and metal−air batteries. Commercially used electrocatalysts for the ORR, such as Pt and Pt/C, are expensive, rare, and not environmentally sustainable. Thus, there is motivation to design materials with the ability to catalyze the ORR that do not incur such high costs and sacrifice resources. Metal oxides have gained a certain prominence in this field with their ease and versatility of preparation, high activity, wide stability range, and environmental abundance. This includes, but is not limited to, perovskites, e.g., $La_{0.5}Sr_{0.5}Co_{0.8}Fe_{0.2}O_3$,[1] spinels, e.g., $Ni_xCo_{3-x}O_4$,[2] and manganese-based oxides, e.g., MnO_2[3] and Mn_2O_3.[4,5] Manganese oxides (MnO_x) have specific advantages in being extremely abundant and are naturally effective at decomposing peroxide,[6] a possible intermediate/product of the ORR. Formally, the ORR can either proceed by a direct, four-electron reduction to hydroxide (eq 1) or a two-electron reduction to peroxide (eq 2), followed by either another two-electron reduction of the peroxide (eq 3) or catalytic decomposition of the peroxide (eq 4).

$$O_2(g) + 2H_2O(l) + 4e^- \rightarrow 4OH^-(aq) \quad (1)$$

$$O_2(g) + H_2O(l) + 2e^- \rightarrow HO_2^-(aq) + OH^-(aq) \quad (2)$$

$$HO_2^-(aq) + H_2O(l) + 2e^- \rightarrow 3OH^-(aq) \quad (3)$$

$$2HO_2^-(aq) \rightarrow 2OH^-(aq) + O_2(g) \quad (4)$$

Blending metal oxides, including MnO_x, with carbon has been shown to greatly increase the preference of the four-electron mechanism due to improved conductivity and electron transport.[7−9] The discovery and implementation of graphene in the past ten years has greatly expanded the possibilities of composite graphene/metal oxide catalysts because of its conductivity,[10] structural variability (e.g., nanoribbons, fullerenes, sheets), effective dispersion of nanomaterials,[3,11] and independent ORR activity.[12] A class of materials that is often overlooked when considering the approaches to increasing conductivity is intrinsically conductive polymers (ICPs), despite the fact that conjugated polymers and polyheterocycles have exhibited extremely high conductivity.

Poly(3,4-ethylenedioxythiophene) (PEDOT) was discovered in the 1980s and has since been utilized in many industries due to its ease of synthesis, high conductivity, optical properties, and stability in humidity and high temperatures. PEDOT can be easily prepared by "in situ" chemical or electrochemical oxidation methods from the 3,4-ethylenedioxythiophene (EDOT) monomer, and is highly conductive when prepared

Received: August 19, 2015
Accepted: October 7, 2015
Published: October 7, 2015

DOI: 10.1021/acsami.5b07684
ACS Appl. Mater. Interfaces 2015, 7, 22745−22750

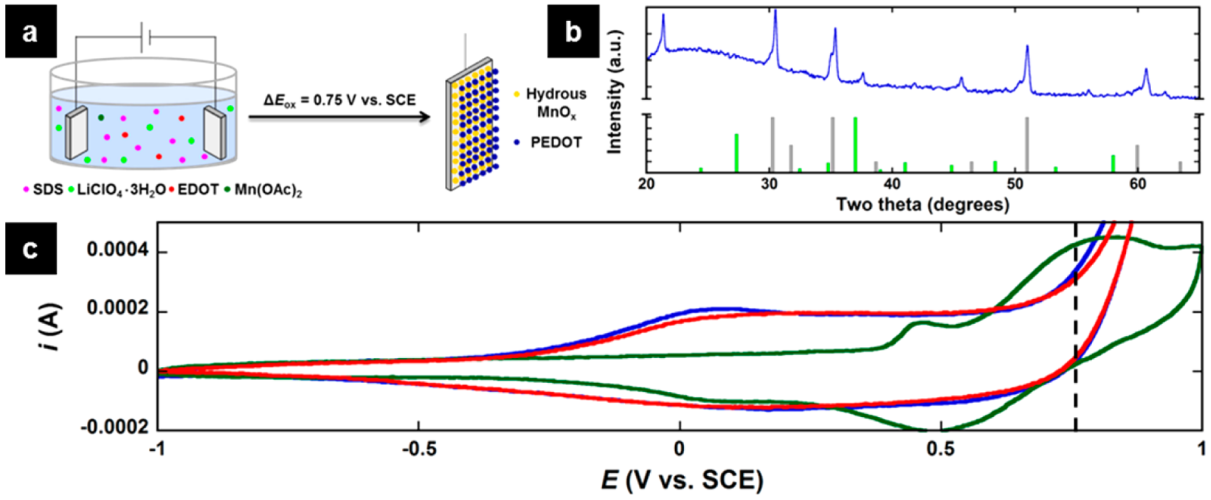

Figure 1. (a) Schematic of the electrodeposition of MnO_x/PEDOT composite thin films; (b) XRD spectra of the MnO_x/PEDOT film grown on ITO, with indices for MnO_2 (green, PDF #053−0633) and background ITO (gray, PDF #039−1058); (c) CV scans in electrodeposition solutions for MnO_x (green), PEDOT (red), and MnO_x/PEDOT (blue), dotted line represents the optimum deposition potential, 0.75 V vs SCE.

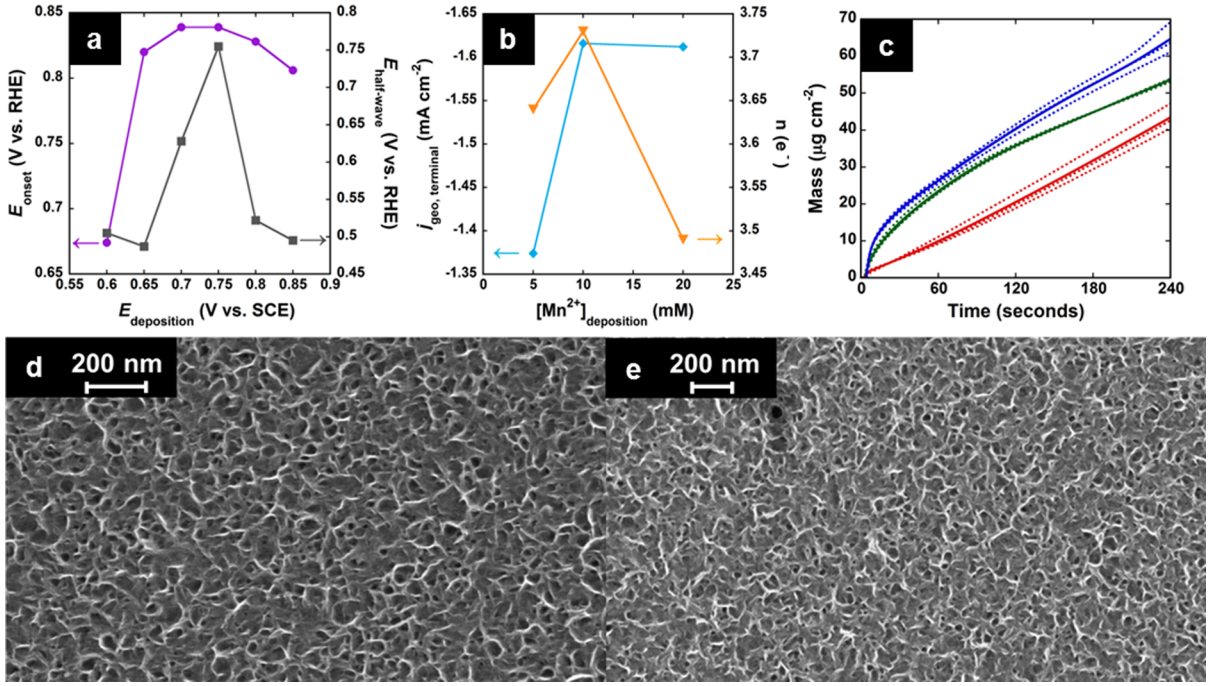

Figure 2. (a) Volcano plot showing the trends in onset potential (purple circles) and half-wave potential (gray squares) as the deposition potential is changed (@ 2500 rpm); (b) Volcano plot showing the trends in terminal current density (blue diamonds) and *n* value (orange triangles) as the Mn^{2+} deposition concentration is changed (@ 2500 rpm); (c) QCM plot showing the mass change vs time of the MnO_x (green), PEDOT (red), and MnO_x/PEDOT (blue) depositions, individual (dotted lines) and average (solid lines) runs; (d) SEM image of a MnO_x/PEDOT film electrodeposited for 40 s; (e) SEM image of a MnO_x/PEDOT film electrodeposited for 120 s.

by either route (~1×10^1 to 1×10^2 S cm^{-1}).[13] Developments by Aaron et al. introduced the possibility of electropolymerization in aqueous media.[14] Besides lowering the oxidation potential, this approach afforded the possibility of coelectrodeposition with other anodically deposited materials, such as MnO_x. The oxidation of Mn^{2+} in solution also occurs at a low potential,[15] making the approach of polymerizing PEDOT and growing a MnO_x film simultaneously very reasonable. Considering the capacitive behavior of both MnO_x and PEDOT alone, the two have been combined successfully for electrochemical capacitors with synergistic behavior.[16−18] MnO_x/PEDOT composites have also been used for catalytic degradation of methylene blue[19] and oxidation of memantine hydrochloride.[20] MnO_x is very often studied for its electrocatalysis of the ORR,[3−5,9,21] but PEDOT has been studied little on its own and as a composite with other metals, metal oxides, and graphene for the ORR.[22−29] To date, few studies have explored the composites of MnO_x and PEDOT for ORR,[29] and a coelectrodeposited film for the ORR has yet to be reported. Herein, we report on the preparation of an electrodeposited MnO_x/PEDOT composite thin film as a highly active catalyst for the oxygen reduction reaction in alkaline electrolyte.

MnO_x/PEDOT composite thin films were electrodeposited by the aqueous micellar route[14] in the presence of Mn^{2+}

DOI: 10.1021/acsami.5b07684
ACS Appl. Mater. Interfaces 2015, 7, 22745−22750

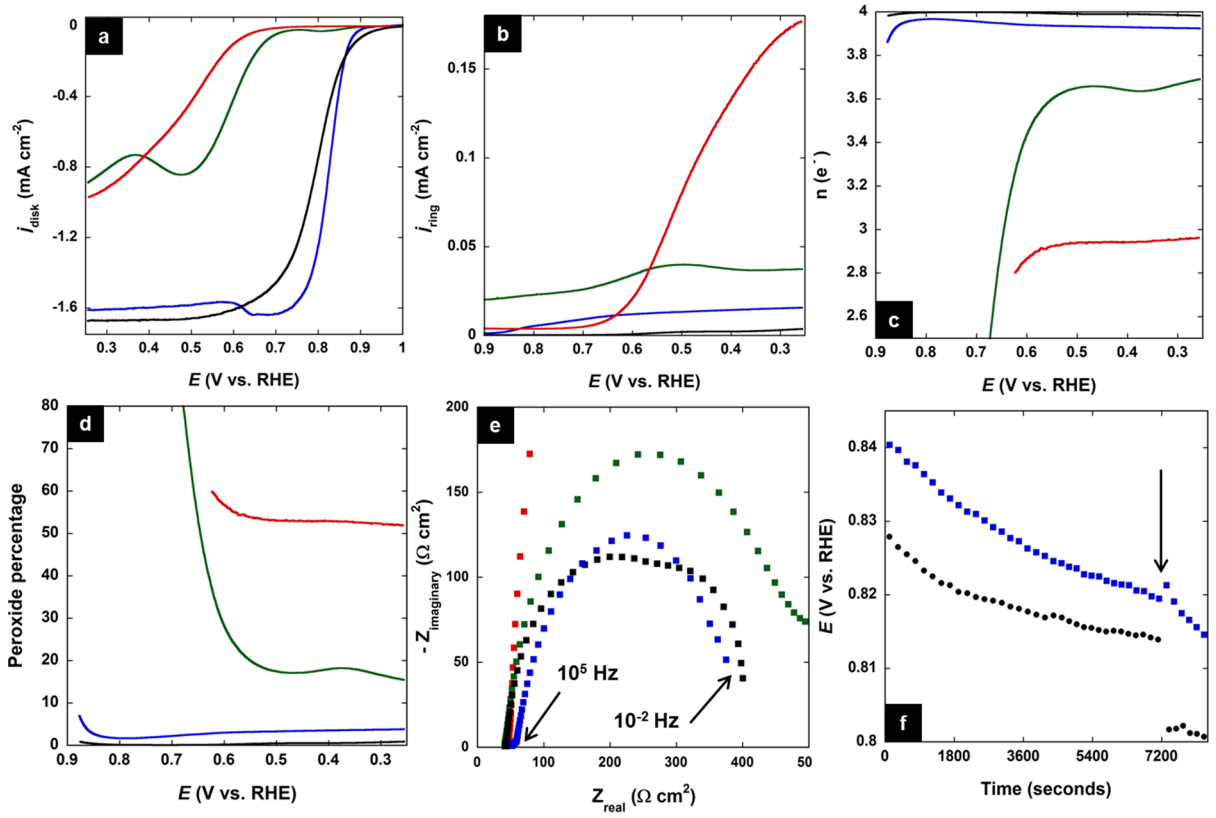

Figure 3. (a) Disk current density LSVs for MnO_x (green), PEDOT (red), MnO_x/PEDOT (blue) and 20% Pt/C (black); (b) Ring current density LSVs for MnO_x, PEDOT, MnO_x/PEDOT and 20% Pt/C; (c) *n* value LSVs for MnO_x, PEDOT, MnO_x/PEDOT and 20% Pt/C; (d) peroxide percentage LSVs for MnO_x, PEDOT, MnO_x/PEDOT and 20% Pt/C; (e) EIS spectra for MnO_x, PEDOT, MnO_x/PEDOT, and 20% Pt/C; (f) stability and methanol experiments on MnO_x/PEDOT and 20% Pt/C, the arrow represents the addition of methanol in to the cell at 2 h. All RDE experiments conducted at 400 rpm.

(Figure 1a), similar to what was reported for preparation of electrochemical capacitors.[16−18] Briefly, MnO_x and PEDOT were coelectrodeposited from an aqueous solution of $Mn(OAc)_2$, EDOT, $LiClO_4$, and sodium dodecyl sulfate (SDS) at an anodic potential. MnO_x only films and PEDOT only films were also electrodeposited, as controls, in the absence of EDOT or $Mn(OAc)_2$, respectively. More detailed accounts of the experimental processes can be found in the Supporting Information. Figure 1b shows that the X-ray diffraction (XRD) spectra of a MnO_x/PEDOT film deposited on indium tin oxide coated glass (ITO, PDF #039−1058) resembles MnO_2 (PDF #053−0633), but with weak intensity. Similarly electrodeposited films of MnO_x have been characterized as MnO_2[17,20] and MnO_x[15,16] in the literature. Here we will refer to the films as hydrous MnO_x.[15] Cyclic voltammetry (CV) was examined in the deposition solutions in order to monitor the redox processes of manganese and EDOT. Figure 1c shows the CV curves, between −1.0 and 1.0 V vs SCE at 100 mV s^{-1}, of the MnO_x, PEDOT, and MnO_x/PEDOT deposition solutions. Two peaks in the anodic scan of MnO_x deposition appear around 0.45 and 0.8 V vs SCE, attributing to a change in Mn valence from 2+ to a mix of 3+ and 4+. Generation of MnO_2 in potentiostatic electrodeposition is proposed to proceed through the generation of bulk Mn^{3+}, which decomposes in to a mix of Mn^{2+} and Mn^{4+}, forming MnO_2 through hydrolysis.[30] Oxidation current of the PEDOT deposition solution begins around −0.25 V vs SCE, corresponding to the oligomerization and polymerization processes at the electrode surface resulting in a thin film, while the rapid current growth beginning at 0.75 V vs SCE is consistent with the oxidation potential of EDOT in aqueous solution.[14] In the combined MnO_x/PEDOT deposition solution, the anodic current of PEDOT coincides with the oxidation processes of manganese.

Because the CV experiments were unclear in providing the optimum oxidation potential for codeposition of MnO_x and PEDOT, films were prepared at varying potentials (0.6 V − 0.85 V, in 0.5 V increments) and their electrocatalytic performance compared utilizing rotating disk electrode (RDE) experiments. Figure 2a shows the trends in ORR metrics of onset potential and half wave potential, as the deposition potential is changed. With the most positive onset (0.84 V) and half-wave (0.75 V) potential values, 0.75 V vs SCE was identified as the deposition potential resulting in the most active MnO_x/PEDOT films and all future composite films were prepared at this potential. The possibility of effecting the MnO_x film growth and performance by changing the concentration of Mn^{2+} in the deposition solution was also investigated. Figure 2b shows the trends in ORR metrics of terminal current density and reaction order (*n* value), as determined from the Koutecky−Levich equation,[2,3,11,21] when the Mn^{2+} concentration was halved (5 mM) and doubled (20 mM). With the highest terminal current density (−1.62 mA cm^{-2}) and *n* value (3.74), 10 mM Mn^{2+} was identified as producing the most active film, and all future composite films were prepared at this concentration.

A quartz crystal microbalance (QCM) was utilized to monitor the changes in film mass during the electrodepositions. Figure 2c shows the resulting mass change over time for the

DOI: 10.1021/acsami.5b07684
ACS Appl. Mater. Interfaces 2015, 7, 22745−22750

electrodeposition of MnO_x, PEDOT, and MnO_x/PEDOT thin films. PEDOT exhibits a near-linear growth rate between 0 and 240 s, while MnO_x and MnO_x/PEDOT show an accelerated rate between 0 and ~30 s followed by a near-linear region between 60 and 240 s. The resemblance of the MnO_x/PEDOT growth to MnO_x is consistent with the qualitative visual observation that the first 30 s of coelectrodeposition is almost completely MnO_x film (gold color) growth, followed by PEDOT polymerization after this initiation period (blue color). QCM was also used to quantify film growth rates, and all of the catalyst films were prepared at an identical mass loading of 40 μg cm^{-2}.

Scanning electron microscopy (SEM) images were taken to examine the morphology of the films and provide further evidence of the coelectrodeposition growth process. Figure 2d,e shows SEM images of MnO_x/PEDOT films grown for 40 and 120 s, respectively. The images show the nanotextured morphology of the films, and that there is no appreciable difference in the overall morphology between 40 and 120 s of deposition. Energy dispersive spectroscopy (EDS) elemental analysis (Figure S1) shows the presence of S and Mn and that their intensity is growing at a linear rate with respect to time. The S present in the film is likely due to both polymer growth and SDS incorporation in to the structure, which is known to occur with the aqueous micellar electropolymerization of PEDOT.[31] Furthermore, cross-sectional analysis indicates that the MnO_x/PEDOT films have average thicknesses of 58, 84, and 111 nm for deposition times of 40, 80, and 120 s, respectively (Figure S2). These values suggest that the films become slightly denser and less porous as the deposition time increases.

Catalyst films were then grown directly on the disk electrode of a rotating ring disk electrode (RRDE) in order to test their electrocatalytic activity toward the ORR. RRDE was used to simultaneously monitor the ORR current at the disk and oxidation current from generated peroxide (if any) at the ring, while scanning from low to high ORR overpotential in O_2-purged and blanketed 0.1 M KOH. It was expected that the MnO_x films would indicate a quasi-four-electron reduction as the intrinsic ability of MnO_x to catalytically decompose peroxide is known.[32,33] PEDOT, while conductive, is generally known to catalyze the ORR by the two-electron mechanism, although there is one example of a vapor phase-polymerized PEDOT operating via a 4-electron ORR process.[28] Co-electrodeposited MnO_x/PEDOT, while used for capacitors, until now has not yet been investigated for electrocatalytic ORR. Figure 3 shows the relevant catalytic ORR data for the electrodeposited films and commercial 20% Pt/C, all at the total mass loading of 40 μg cm^{-2}.

Figure 3a shows the increase in ORR activity from the MnO_x and PEDOT films to the MnO_x/PEDOT composite film. The synergistic effect of the coelectrodeposition can be seen in the improvement in onset potential (MnO_x: 0.682 V vs RHE, PEDOT: 0.622 V, MnO_x/PEDOT: 0.877 V), half-wave potential (MnO_x: 0.593 V vs RHE, PEDOT: 0.481 V, MnO_x/PEDOT: 0.825 V), and terminal current density (MnO_x, −0.892 mA cm^{-2}; PEDOT, −0.971 mA cm^{-2}; MnO_x/PEDOT, −1.617 mA cm^{-2}). Furthermore, the metric values of the MnO_x/PEDOT films are equal to or better than those of commercial benchmark catalyst 20% Pt/C, with an onset potential of 0.875 V vs RHE, a half-wave potential of 0.791 V vs RHE, and a terminal current density of −1.667 mA cm^{-2}. While the onset potential and terminal current values are similar, the MnO_x/PEDOT film (half-wave potential: 0.825 V vs RHE) outperforms 20% Pt/C (half-wave potential: 0.791 V) in the half-wave regime. This distinction is of importance as the half-wave region is generally around the potential in which the maximum power could be extracted from a fuel cell.[34] Tafel slopes were also calculated to assess the kinetic effectiveness of each catalyst in the onset region. A low slope signifies a more effective catalyst; and the slopes trend with the overall ORR activity here, PEDOT (106 mV dec^{-1}) > MnO_x (91 mV dec^{-1}) > 20% Pt/C (87 mV dec^{-1}) > MnO_x/PEDOT (39 mV dec^{-1}). An ORR metric comparison with all other PEDOT and PEDOT composite catalysts studied by RDE can be seen in Table S1. This data shows the superior performance of the MnO_x/PEDOT films prepared here when compared to other PEDOT-based ORR electrocatalysts.

Ring current linear scanning voltammetry (LSV) scans in Figure 3b represent the current from the oxidation of peroxide being generated by the catalysts performing ORR on the disk. The PEDOT and MnO_x control films exhibit significantly higher ring current during the ORR, especially when considered as a ratio of ring/disk current density [(j_R/j_D), where PEDOT j_R/j_D = 0.177, MnO_x j_R/j_D = 0.045, MnO_x/PEDOT j_R/j_D = 0.012, 20% Pt/C j_R/j_D = 0.003]. The quantification of ring and disk current by RRDE allows an accurate calculation of the n value and percent of peroxide generated for each catalyst, based on the collection efficiency of the instrument (see the Supporting Information). n values, $n = 4(I_D)/(I_D+I_R/N)$ where I_D is the disk current, I_R is the ring current, and N is the collection efficiency, are shown in Figure 3c. 20% Pt/C, as expected, showed an n value of ~4 from low (onset, n = 3.98) to high overpotential (steady-state, n = 3.98) as it generally proceeds by an efficient four-electron ORR mechanism. MnO_x/PEDOT exhibited a quasi-four-electron ORR mechanism, perhaps two rapid two electron transfers, with an essentially constant n value from low (onset, n = 3.86) to high overpotential (steady-state, n = 3.92). These values demonstrate the remarkable synergism between MnO_x and PEDOT as the maximum attained n values for these catalysts individually were 3.68 and 2.96, respectively. Hence, the peroxide generation (Figure 3d), $\%(H_2O_2) = 200(I_R/N)/(I_R/N+I_D)$, of the MnO_x/PEDOT film was significantly lower (<5%) at all overpotentials than the MnO_x (>15%) and PEDOT (>50%) films. 20% Pt/C generated <1% peroxide, further verifying its efficient reduction of oxygen.

Considering the similarity of the MnO_x/PEDOT film and 20% Pt/C in ORR activity, further testing was done to assess their charge transfer and stability characteristics. Electrochemical Impedance Spectroscopy (EIS) experiments were carried out at constant half-wave current in O_2-purged and blanketed 0.1 M KOH, Figure 3e. Modeling to the equivalent Randles circuit yielded charge transfer resistance (R_{CT}) values of 361 Ω (MnO_x/PEDOT), 394 Ω (20% Pt/C), 478 Ω (MnO_x), and 3117 Ω (PEDOT). R_{CT} values calculated in the onset region of the ORR LSV yielded the same trend: 806 Ω (MnO_x/PEDOT), 1181 Ω (20% Pt/C), 2215 Ω (MnO_x), and 2997 Ω (PEDOT). Co-electrodeposition of MnO_x and PEDOT clearly helps facilitate electron transfer during the ORR, perhaps even more efficiently than the 20% Pt/C benchmark catalyst. The intimate electrode contact realized by electrodeposition could explain the low resistances, another fundamental and practical advantage over a commercial powder electrocatalyst. Galvanostatic stability experiments were also carried out at constant half-wave current in O_2-purged and

DOI: 10.1021/acsami.5b07684
ACS Appl. Mater. Interfaces 2015, 7, 22745−22750

blanketed 0.1 M KOH for 8400 s, Figure 3f. The MnO_x/PEDOT and 20% Pt/C catalysts were extremely stable over a 2 h period, both retaining >97% of their activity. After 2 h, methanol (5 wt %) was introduced in order to test the catalysts' electrocatalytic selectivity for ORR in the presence of methanol (arrow, Figure 3f). The MnO_x/PEDOT film displayed higher tolerance for methanol than 20% Pt/C suggesting its compatibility with methanol fuel cells. Combined with the fact that PEDOT has been used in fuel cells to limit methanol crossover[34] and as a catalyst support,[35] the development of MnOx/PEDOT could find real application as an electrocatalyst in fuel cells.

In summary, MnO_x/PEDOT composite thin films were anodically electrodeposited by an aqueous micellar route and used as electrocatalysts for the ORR. The composite MnO_x/PEDOT thin film showed significant improvements over the MnO_x and PEDOT control films for the ORR: 0.2−0.25 V more positive onset potential, 0.23−0.34 V more positive half-wave potential, 0.6−0.7 mA cm^{-2} increase in terminal current density, and 100−2700 Ω decrease in R_{CT}, as studied here. The activity of the MnO_x/PEDOT proved competitive with the commercial benchmark catalyst 20% Pt/C in terms of onset potential (MnO_x/PEDOT, 0.877 V vs RHE;, 20% Pt/C, 0.875 V), half-wave potential (MnO_x/PEDOT, 0.825 V vs RHE; 20% Pt/C, 0.791 V), R_{CT} (MnO_x/PEDOT, 361 Ω; 20% Pt/C, 394 Ω), and exhibited superior electrocatalytic selectivity for ORR when exposed to methanol. The synergism and high activity of the MnO_x/PEDOT film is attributed to the facilitated electron transport, realized by coelectrodepositing MnO_x and PEDOT.

■ ASSOCIATED CONTENT

Supporting Information

The Supporting Information is available free of charge on the ACS Publications website at DOI: 10.1021/acsami.5b07684.

Additional experimental details, figures, and tables (PDF)

■ AUTHOR INFORMATION

Corresponding Author

*E-mail: tnlambe@sandia.gov. Fax: 505 844 7786. Tel: 505 284 6967.

Author Contributions

The manuscript was written through contributions of all authors. All authors have given approval to the final version of the manuscript.

Notes

The authors declare no competing financial interest.

Current metal prices: Mn, 1.78 USD/kg; Pt, 30900 USD/kg. Mn is ∼17 000× cheaper than Pt. (From http://www.infomine.com/investment/). Onset potential values were calculated by the tangential method (see the Supporting Information).

■ ACKNOWLEDGMENTS

This work was supported by the Laboratory Directed Research and Development program at Sandia National Laboratories, a multiprogram laboratory managed and operated by Sandia Corporation, a wholly owned subsidiary of Lockheed Martin Corporation, for the U.S. Department of Energy's National Nuclear Security Administration, under contract DE-AC04-94AL85000. Ms. Bonnie McKenzie is thanked for her technical assistance with SEM imaging and EDS elemental analysis.

■ REFERENCES

(1) Park, H. W.; Lee, D. U.; Zamani, P.; Seo, M. H.; Nazar, L. F.; Chen, Z. Electrospun Porous Nanorod Perovskite Oxide/Nitrogen-Doped Graphene Composite as a Bi-Functional Catalyst for Metal Air Batteries. *Nano Energy* **2014**, *10*, 192−200.

(2) Lambert, T. N.; Vigil, J. A.; White, S. E.; Davis, D. J.; Limmer, S. J.; Burton, P. D.; Coker, E. N.; Beechem, T. E.; Brumbach, M. T. Electrodeposited $Ni_xCo_{3-x}O_4$ Nanostructured Films as Bifunctional Oxygen Electrocatalysts. *Chem. Commun.* **2015**, *51* (46), 9511−9514.

(3) Lambert, T. N.; Davis, D. J.; Lu, W.; Limmer, S. J.; Kotula, P. G.; Thuli, A.; Hungate, M.; Ruan, G.; Jin, Z.; Tour, J. M. Graphene-Ni-α-MnO_2 and -Cu-α-MnO_2 Nanowire Blends as Highly Active Non-Precious Metal Catalysts for the Oxygen Reduction Reaction. *Chem. Commun.* **2012**, *48* (64), 7931−7933.

(4) Su, H.-Y.; Gorlin, Y.; Man, I. C.; Calle-Vallejo, F.; Norskov, J. K.; Jaramillo, T. F.; Rossmeisl, J. Identifying Active Surface Phases for Metal Oxide Electrocatalysts: a Study of Manganese Oxide Bi-Functional Catalysts for Oxygen Reduction and Water Oxidation Catalysis. *Phys. Chem. Chem. Phys.* **2012**, *14* (40), 14010−14022.

(5) Gorlin, Y.; Jaramillo, T. F. A Bifunctional Nonprecious Metal Catalyst for Oxygen Reduction and Water Oxidation. *J. Am. Chem. Soc.* **2010**, *132* (39), 13612−13614.

(6) Hasan, M. A.; Zaki, M. I.; Pasupulety, L.; Kumari, K. Promotion of the Hydrogen Peroxide Decomposition Activity of Manganese Oxide Catalysts. *Appl. Catal., A* **1999**, *181* (1), 171−179.

(7) Kim, H.; Popov, B. N. Synthesis and Characterization of MnO_2-Based Mixed Oxides as Supercapacitors. *J. Electrochem. Soc.* **2003**, *150* (3), D56−D62.

(8) Zhang, L. L.; Wei, T.; Wang, W.; Zhao, X. S. Manganese Oxide−Carbon Composite as Supercapacitor Electrode Materials. *Microporous Mesoporous Mater.* **2009**, *123* (1−3), 260−267.

(9) Lee, J.-S.; Lee, T.; Song, H.-K.; Cho, J.; Kim, B.-S. Ionic Liquid Modified Graphene Nanosheets Anchoring Manganese Oxide Nanoparticles as Efficient Electrocatalysts for Zn-Air Batteries. *Energy Environ. Sci.* **2011**, *4* (10), 4148−4154.

(10) Marinho, B.; Ghislandi, M.; Tkalya, E.; Koning, C. E.; de With, G. Electrical Conductivity of Compacts of Graphene, Multi-Wall Carbon Nanotubes, Carbon Black, and Graphite Powder. *Powder Technol.* **2012**, *221*, 351−358.

(11) Davis, D. J.; Raji, A.-R. O.; Lambert, T. N.; Vigil, J. A.; Li, L.; Nan, K.; Tour, J. M. Silver-Graphene Nanoribbon Composite Catalyst for the Oxygen Reduction Reaction in Alkaline Electrolyte. *Electroanalysis* **2014**, *26* (1), 164−170.

(12) Wang, S.; Zhang, L.; Xia, Z.; Roy, A.; Chang, D. W.; Baek, J.-B.; Dai, L. BCN Graphene as Efficient Metal-Free Electrocatalyst for the Oxygen Reduction Reaction. *Angew. Chem., Int. Ed.* **2012**, *51* (17), 4209−4212.

(13) Elschner, A.; Kirchmeyer, S.; Lovenich, W.; Merker, U.; Reuter, K. *PEDOT: Principles and Applications of an Intrinsically Conductive Polymer*; CRC Press: Boca Raton, FL, 2010.

(14) Sakmeche, N.; Aaron, J. J.; Fall, M.; Aeiyach, S.; Jouini, M.; Lacroix, J. C.; Lacaze, P. C. Anionic Micelles; a New Aqueous Medium for Electropolymerization of Poly(3,4-ethylenedioxythiophene) Films on Pt Electrodes. *Chem. Commun.* **1996**, *24*, 2723−2724.

(15) Tench, D.; Warren, L. F. Electrodeposition of Conducting Transition Metal Oxide/Hydroxide Films from Aqueous Solution. *J. Electrochem. Soc.* **1983**, *130* (4), 869−872.

(16) Babakhani, B.; Ivey, D. G. Improved Capacitive Behavior of Electrochemically Synthesized Mn Oxide/PEDOT Electrodes Utilized as Electrochemical Capacitors. *Electrochim. Acta* **2010**, *55* (12), 4014−4024.

(17) Liu, R.; Lee, S. B. MnO_2/Poly(3,4-ethylenedioxythiophene) Coaxial Nanowires by One-Step Coelectrodeposition for Electrochemical Energy Storage. *J. Am. Chem. Soc.* **2008**, *130* (10), 2942−2943.

(18) Tang, P.; Zhao, Y.; Xu, C. Step-by-Step Assembled Poly(3,4-ethylenedioxythiophene)/Manganese Dioxide Composite Electrodes: Tuning the Structure for High Electrochemical Performance. *Electrochim. Acta* **2013**, *89*, 300−309.

DOI: 10.1021/acsami.5b07684
ACS Appl. Mater. Interfaces 2015, 7, 22745−22750

(19) Zhang, L.; Jamal, R.; Zhao, Q.; Wang, M.; Abdiryim, T. Preparation of PEDOT/GO, PEDOT/MnO2, and PEDOT/GO/MnO2 Nanocomposites and Their Application in Catalytic Degradation of Methylene Blue. *Nanoscale Res. Lett.* **2015**, *10* (1), 1−9.
(20) Wu, Z. Y.; Thiagarajan, S.; Chen, S. M.; Lin, K. C. Electrochemical Preparation and Characterization of MnO_2-PEDOT Hybrid Film and its Application in Electrocatalytic Oxidation of Memantine Hydrochloride. *Int. J. Electrochem. Sci.* **2012**, *7* (2), 1230−1241.
(21) Davis, D. J.; Lambert, T. N.; Vigil, J. A.; Rodriguez, M. A.; Brumbach, M. T.; Coker, E. N.; Limmer, S. J. Role of Cu-Ion Doping in Cu-α-MnO_2 Nanowire Electrocatalysts for the Oxygen Reduction Reaction. *J. Phys. Chem. C* **2014**, *118* (31), 17342−17350.
(22) Cottis, P. P.; Evans, D.; Fabretto, M.; Pering, S.; Murphy, P.; Hojati-Talemi, P. Metal-Free Oxygen Reduction Electrodes Based on Thin PEDOT Films with High Electrocatalytic Activity. *RSC Adv.* **2014**, *4* (19), 9819−9824.
(23) Ma, J.; Xue, T.; Zou, Z.; Wang, B.; Luo, M. Improved Oxygen Reduction Activity on PEDOT Via Electroolymerisation In Ionic Liquid. *Int. J. Electrochem. Sci.* **2015**, *10*, 4562−4570.
(24) Guo, Z.; Qiao, Y.; Liu, H.; Ding, C.; Zhu, Y.; Wan, M.; Jiang, L. Self-Assembled Hierarchical Micro/Nano-Structured PEDOT as an Efficient Oxygen Reduction Catalyst Over a Wide pH Range. *J. Mater. Chem.* **2012**, *22* (33), 17153−17158.
(25) Zhang, M.; Yuan, W.; Yao, B.; Li, C.; Shi, G. Solution-Processed PEDOT:PSS/Graphene Composites as the Electrocatalyst for Oxygen Reduction Reaction. *ACS Appl. Mater. Interfaces* **2014**, *6* (5), 3587−3593.
(26) Guo, Z.; Jiang, C.; Teng, C.; Ren, G.; Zhu, Y.; Jiang, L. Sulfur, Trace Nitrogen and Iron Codoped Hierarchically Porous Carbon Foams as Synergistic Catalysts for Oxygen Reduction Reaction. *ACS Appl. Mater. Interfaces* **2014**, *6* (23), 21454−21460.
(27) Guo, Z.; Liu, H.; Jiang, C.; Zhu, Y.; Wan, M.; Dai, L.; Jiang, L. Biomolecule-Doped PEDOT with Three-Dimensional Nanostructures as Efficient Catalyst for Oxygen Reduction Reaction. *Small* **2014**, *10* (10), 2087−2095.
(28) Winther-Jensen, B.; Winther-Jensen, O.; Forsyth, M.; MacFarlane, D. R. High Rates of Oxygen Reduction over a Vapor Phase−Polymerized PEDOT Electrode. *Science* **2008**, *321* (5889), 671−674.
(29) Chowdhury, A. D.; Agnihotri, N.; Sen, P.; De, A. Conducting $CoMn_2O4$ - PEDOT Nanocomposites as Catalyst in Oxygen Reduction Reaction. *Electrochim. Acta* **2014**, *118*, 81−87.
(30) Das, D.; Sen, P. K.; Das, K. Mechanism of Potentiostatic Deposition of MnO_2 and Electrochemical Characteristics of the Deposit in Relation to Carbohydrate Oxidation. *Electrochim. Acta* **2008**, *54* (2), 289−295.
(31) Sakmeche, N.; Aeiyach, S.; Aaron, J.-J.; Jouini, M.; Lacroix, J. C.; Lacaze, P.-C. Improvement of the Electrosynthesis and Physicochemical Properties of Poly(3,4-ethylenedioxythiophene) Using a Sodium Dodecyl Sulfate Micellar Aqueous Medium. *Langmuir* **1999**, *15* (7), 2566−2574.
(32) Benbow, E. M.; Kelly, S. P.; Zhao, L.; Reutenauer, J. W.; Suib, S. L. Oxygen Reduction Properties of Bifunctional α-Manganese Oxide Electrocatalysts in Aqueous and Organic Electrolytes. *J. Phys. Chem. C* **2011**, *115* (44), 22009−22017.
(33) Mao, L.; Zhang, D.; Sotomura, T.; Nakatsu, K.; Koshiba, N.; Ohsaka, T. Mechanistic Study of the Reduction of Oxygen in Air Electrode with Manganese Oxides as Electrocatalysts. *Electrochim. Acta* **2003**, *48* (8), 1015−1021.
(34) Stanis, R. J.; Lambert, T. N.; Yaklin, M. A. Poly(3,4-ethylenedioxythiphene) (PEDOT)-Modified Anodes: Reduced Methanol Crossover in Direct Methanol Fuel Cells. *Energy Fuels* **2010**, *24* (5), 3125−3129.
(35) Tintula, K. K.; Sahu, A. K.; Shahid, A.; Pitchumani, S.; Sridhar, P.; Shukla, A. K. Directed Synthesis of MC-PEDOT Composite Catalyst-Supports for Durable PEFCs. *J. Electrochem. Soc.* **2011**, *158* (6), B622−B631.

DOI: 10.1021/acsami.5b07684
ACS Appl. Mater. Interfaces 2015, 7, 22745−22750